MECHANIKA TEORETYCZNA
I STOSOWANA
Journal of Theoretical
and Applied Mechanics
3, 34, 1996

SECOND MODE INSTABILITY

EWA TULISZKA-SZNITKO

Institute of Thermal Engineering Technical University of Poznań

e-mail: sznitko@orion.tup.edu.pl

Stability characteristics of the second mode waves are investigated theoretically. Numerical results are compared with the experimental data of Stetson. The sensitivity of calculated amplification rates of disturbances to various physical parameters (viscosity-temperature law, thermal boundary conditions, Stokes hypothesis) is tested.

Key words: instability, laminar-turbulent transition

1. Introduction

The successful design of the future hypersonic vehicle demands an accurate determination of the whole transition process from laminar to the turbulent boundary layer state. Prevention or delay of transition has the dual benefits of reducing both the viscous drag and surface heating resulting, among other things, in increased payloads and less stringent material requirements. It is known that various factors influence the location and extent of the transition zone. Among these are surface roughness, acoustic waves, free stream turbulence and bluntness of a body. The boundary layer stability theory provides means for studying the effects of various control parameters on transition. Every theoretical method for transition prediction must be verified by experimental results; therefore it is very important to improve both the theoretical and experimental method in order to minimize their errors. In the present paper numerical calculations are made to find how sensitive are the calculated amplification rates of disturbances in laminar boundary layer to variations of physical parameters and precision of theoretical modeling of the stability problem. Calculations made for hypersonic flow (where the so-called second mode waves are dominant) are compared with the experimental data of Stetson et

al. (1983) and the theoretical results of Simen and Dallmann (1992) and Mack (1987).

Experiments which make possible a direct comparison between spatial amplification rates of disturbances obtained from the linear stability theory and those obtained from measurements were carried out at supersonic flow on flat plates by Demetriades (1960), Laufer and Vrebolovich (1960), Kosinov et al. (1989), (1990), Kendall (1967) and for a sharp cone of zero angle of attack at hypersonic flow by Kendall (1975), Demetriades (1977) and Stetson et al. (1983). The largest number of results and the best description were given by Stetson. This was the main reason for taking Stetson's data as a reference for comparison between theory and experiment. Additionally, a cone geometry (used by Stetson) is closer to the practical configuration than a flat plate.

The stability analysis used here is based on the linear, local primary stability theory. Using the local linear theory we neglect such physical effects as: receptivity, nonlinearity, interaction of disturbances, non-parallel flow and bluntness of the body, so we cannot expect that the calculated instability characteristics reflect exactly the experimental data. However, the inaccuracy due to theoretical simplification made in the linear stability theory is considered to be small enough to draw reliable qualitative conclusions out of the results.

2. Second mode instability

As mentioned in Section 1, in hypersonic boundary layer the second mode waves are dominating. The stability theory of Lees and Lin (1946), Lees and Roshodko (1962) and the theory of Mack (1963), (1964), (1965), which established the existence of unstable higher modes, have important consequences for the instability of supersonic and hypersonic boundary layer.

Lees and Lin classified the instability waves as:

– subsonic

$$U_e - c < a_e \qquad \frac{U_e - c}{a_e} = \overline{\mathrm{Ma}_e} < 1$$

– sonic

$$U_e - c = a_e \qquad \frac{U_e - c}{a_e} = \overline{\mathrm{Ma}_e} = 1$$

– supersonic

$$U_e - c > a_e \qquad \frac{U_e - c}{a_e} = \overline{\mathrm{Ma}_e} > 1$$

where

U – velocity

a – speed of sound

c – phase speed of the wave

$\overline{\mathrm{Ma}_e}$ – Mach number of free stream flow relative to the phase velocity

and e denotes boundary layer edge values.

Neutral supersonic waves are the Mach waves of relative flow, and can exist as either outgoing or incoming waves. Almost all the true instability waves, which satisfy the boundary condition at the wall and at infinity, are subsonic. Only subsonic waves are considered in this paper.

Lees and Lin showed that the necessary and sufficient condition for existence of neutral and unstable wave in inviscid boundary layer is that there is a point $y_s > y_0$ (so-called the generalized inflection point) in the boundary layer where

$$\frac{d}{dy}\left(\frac{\rho dU}{dy}\right) = 0 \tag{2.1}$$

y – coordinate perpendicular to the wall

0 – point at which dimensionless velocity $U/U_e = 1 - 1/\mathrm{Ma}$

ρ – density.

The Lees and Lin proof requires the local relative Much number to be subsonic everywhere $\overline{\mathrm{Ma}}^2 < 1$ ($\overline{\mathrm{Ma}} = (U - c)/a = \mathrm{Ma} - c/a$). If $\overline{\mathrm{Ma}}^2 < 1$ everywhere in the boundary layer there is a unique wave number corresponding to the phase speed of neutral wave.

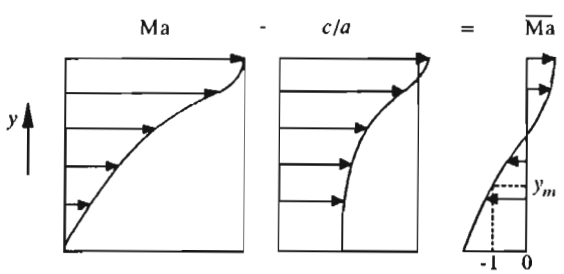

Fig. 1. Distribution scheme of the relative Mach number in boundary layer

Mack demonstated the existence of higher modes for inviscid, two-dimensional stability equations which evidently have a different analytical character depending on whether the relative Mach number $\overline{\mathrm{Ma}}^2$ is less or

greater than 1. In Fig.1 a schematic picture of the distributions of local Mach number, phase speed ratio to the local speed of sound c/a (phase speed is constant but the local speed of sound is a function of y) and the resulting relative Mach number $\overline{\mathrm{Ma}}$ in a typical hypersonic boundary layer is shown. If the local relative Mach number is supersonic $\overline{\mathrm{Ma}}^2 > 1$, say between $y = 0$ and $y = y_m$ (Fig.1), the mathematical nature of stability equations changes. The equations are elliptic for $\overline{\mathrm{Ma}}^2 < 1$ and become the wave equations for $\overline{\mathrm{Ma}} > 1$ and, as in all problems governed by the wave equations, there is an infinite sequence of solutions that will satisfy the boundary conditions. From the sequence of solutions, only the first two are important, the so-called first and second modes. The second mode which is expected to play a dominant role in the transition process in hypersonic flow differs consideriably from the first mode instability.

For a boundary layer edge Mach number smaller than about four, the major instabilities are expected to be those associated with the first mode. These first modes in two-dimensional compressible flow (Tollmien-Schlichting type waves) are most unstable for obliqueness angles of $\gamma = 40 \div 60$ degrees ($\gamma = \arctan(\alpha/beta)$, α, β are the wave angle components) and are stabilized by cooling. The first modes in three-dimensional boundary layers are stabilized by wall cooling but this effect decreases with the increasing crossflow velocity component.

In both two and three-dimensional boundary layers the second mode waves are the two-dimensional waves. They are destabilized by wall cooling (which is shown in Section 5).

The stabilizing effect of cooling on the first mode is said to be due to a movement of generalized inflexion point within the boundary layer towards the wall. Solutions obtained from the cone boundary layer equations for $\mathrm{Ma} = 6.8$ and for different wall temperatures are shown in Fig.2 (δ is the boundary layer thicknes, ζ is the coordinate perpendicular to the cone – Fig.4). For adiabatic condition ($T_w/T_{ad} = 1.0$) the generalized inflexion point corresponds to the maximum value of $\rho dU/d\zeta$ and is located near the boundary layer outer edge. As cooling is applied, a second generalized inflexion point appears close to the wall; at this point $\rho dU/d\zeta$ is minimum. With increasing cooling, the second generalized inflexion point moves outwards, whereas the altitude of the first one decreases slightly. At a certain temperature inflexion points join each other and finally both of them disappear.

Cooling does not stabilize second modes because their existence is independent of location of the inflexion point; it depends only on the existence of supersonic range within the boundary layer where $\overline{\mathrm{Ma}}^2 > 1$. Fig.3 illustrates

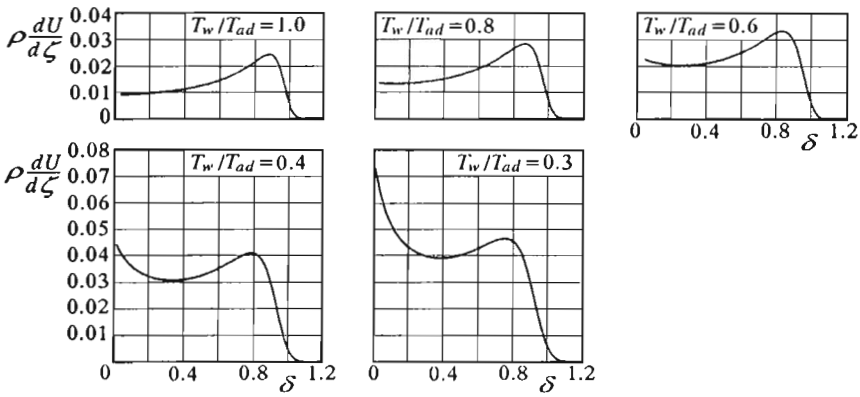

Fig. 2. Distribution of $\rho dU/d\zeta$ in boundary layer for different wall thermal conditions

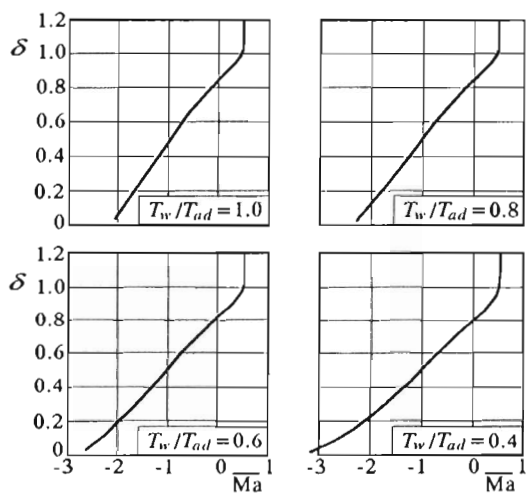

Fig. 3. Distribution of the relative Mach number for different wall thermal conditions; $\mathrm{Ma}_e = 6.8$

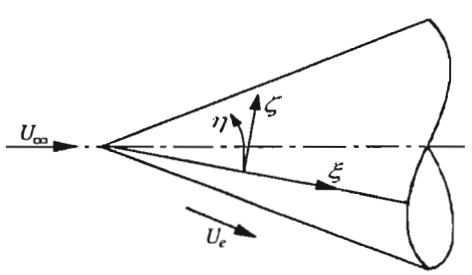

Fig. 4. Scheme of curvelinear coordinate system

the distribution of relative Mach number $\overline{\mathrm{Ma}}$ in the boundary layer. Calculations were made for the same geometry and edge Mach number as in Fig.2. From Fig.3 we can see that with increasing cooling the supersonic range of boundary layer becomes larger and consequently the boundary layer becomes more unstable.

3. Formulation of the problem

The evolution of disturbances in compressible boundary layers is governed by the compressible continuity equation, Navier-Stockes equation and energy equation

$$\frac{\partial \rho}{\partial t} + \nabla \cdot (\rho \boldsymbol{V}) = 0$$

$$\rho\Big[\frac{\partial \boldsymbol{V}}{\partial t} + (\boldsymbol{V} \cdot \nabla)\boldsymbol{V}\Big] = -\nabla p - \nabla \times [\mu(\nabla \times \boldsymbol{V})] + \nabla[(\lambda + 2\mu)\nabla \cdot \boldsymbol{V}] \quad (3.1)$$

$$\rho c_p\Big[\frac{\partial T}{\partial t} + (\boldsymbol{V} \cdot \nabla)T\Big] = \nabla \cdot (k\nabla T) + \frac{\partial p}{\partial t} + (\boldsymbol{V} \cdot \nabla)p + \Phi$$

where

$\boldsymbol{V}$ – velocity vector
ρ – density
p – pressure
T – temperature
c_p – specific heat under constant pressure
k – termal conductivity
μ, λ – first and second coefficients of viscosity, respectively.

The viscous dissipation function is given as

$$\Phi = \lambda(\nabla \cdot \boldsymbol{V})^2 + \frac{\mu}{2}(\nabla \boldsymbol{V} + \nabla \boldsymbol{V}^{\mathrm{T}})^2 \quad (3.2)$$

The equation of state is given by the perfect gas relation

$$p = \rho \tilde{R} T \quad (3.3)$$

It can be well assumed that under the considered conditions of free stream Mach number up to eight and wall temperature up to 800 K the perfect gas assumption is still valid (a typical case of chemical reactions appearance in the

flow is Mach number about twenty five and the wall temperature of 1200 K; Simen and Dallmann (1992)).

In this research, we formulate the compressible stability problem in the body oriented coordinate system (ξ, ζ, η) shown in Fig.4. The coordinates ξ, ζ, η represent the streamwise, wall-normal and spanwise directions, respectively. All the lengths are scaled by a viscous scale $\sqrt{\nu\xi/U_e}$, velocity by U_e, density by ρ_e, pressure by $\rho_e U_e^2$, time by $\sqrt{\nu\xi/U_e}/U_e$ and other variables by the corresponding boundary-layer edge values denoted by e. The flow is perturbed by fluctuations in the flow, therefore the total field can be decomposed into its mean value $(U, V, W, P, T, \rho_0, K, \mu_0, \lambda_0)$ and a perturbation $(u', v', w', p', \tau', \rho', k', \mu', \lambda')$

$$\begin{array}{lll} u = U + u' & v = V + v' & w = W + w' \\ p = P + p' & \tau = T + \tau' & \rho = \rho_0 + \rho' \\ k = K + k' & \mu = \mu_0 + \mu' & \lambda = \lambda_0 + \lambda' \end{array} \tag{3.4}$$

where u, v, w are velocity components in ξ, ζ, η directions respectively.

Substituting Eq (3.4) into the Navier-Stokes equations, subtracting from the governing equations those corresponding to the steady mean flow, and using the equation of state, we obtain the governing equations for the disturbances as

$$\begin{aligned} &\mathbf{F}\frac{\partial \boldsymbol{\Psi}}{\partial t} + \mathbf{A}\frac{\partial \boldsymbol{\Psi}}{\partial \xi} + \mathbf{B}\frac{\partial \boldsymbol{\Psi}}{\partial \zeta} + \mathbf{C}\frac{\partial \Psi}{\partial \eta} + \mathbf{D}\boldsymbol{\Psi} = \\ &= \mathbf{H}_{\xi\xi}\frac{\partial^2 \boldsymbol{\Psi}}{\partial \xi^2} + \mathbf{H}_{\xi\zeta}\frac{\partial^2 \boldsymbol{\Psi}}{\partial \xi \partial \zeta} + \mathbf{H}_{\zeta\zeta}\frac{\partial^2 \boldsymbol{\Psi}}{\partial \zeta^2} + \mathbf{H}_{\xi\eta}\frac{\partial^2 \Psi}{\partial \xi \partial \eta} + \mathbf{H}_{\zeta\eta}\frac{\partial^2 \boldsymbol{\Psi}}{\partial \zeta \partial \eta} + \mathbf{H}_{\eta\eta}\frac{\partial^2 \boldsymbol{\Psi}}{\partial \eta^2} \end{aligned} \tag{3.5}$$

where $\boldsymbol{\Psi}$ is defined as

$$\boldsymbol{\Psi} = [u', v', w', \tau', p']^{\mathsf{T}} \tag{3.6}$$

Matrices $\mathbf{F}$, $\mathbf{A}$, $\mathbf{B}$, $\mathbf{C}$, $\mathbf{D}$, $\mathbf{H}_{\xi\xi}$, $\mathbf{H}_{\xi\zeta}$, $\mathbf{H}_{\zeta\zeta}$, $\mathbf{H}_{\xi\eta}$, $\mathbf{H}_{\zeta\eta}$ and $\mathbf{H}_{\eta\eta}$ are decomposed following Chang and Malik (1991), (1993) to a linear part with only mean flow quantities (denoted by superscripts l) and the nonlinear one which contains mean flow and perturbation quantities (denoted by n). For instance

$$\mathbf{F} = \mathbf{F}^n + \mathbf{F}^l \tag{3.7}$$

The governing PDEs of disturbances are hyperbolic in time and elliptic in the streamwise direction. To solve such a system of equations we must know the outflow boundary condition which is very difficult to predict. However, with appropriate simplification the equations could be parabolized. Herbert

(1991) and Bertolotti (1991) described ways of parabolizing the governing PDEs.

Following the linear theory (neglecting nonlinear terms in Eqs (3.5) and restricting ourselves to axisymmetric bodies) we assume that the disturbance vector $\boldsymbol{\Psi}$ can be expressed as

$$\boldsymbol{\Psi}(\xi,\zeta,\eta,t) = \overline{\boldsymbol{\Psi}}(\xi,\zeta)\exp\Big[\mathrm{i}\Big(\int_{\xi_0}^{\xi}\alpha(\xi)\,d\xi + m\eta - \omega t\Big)\Big] \tag{3.8}$$

where $\overline{\boldsymbol{\Psi}}(\xi,\zeta)$ stands for the complex amplitude function. The wave angle is expressed as

$$\gamma = \arctan\Big(\frac{m}{R}\alpha\Big) \tag{3.9}$$

where $R = h_\eta$ is the Lame parameter.

After introducing Eq (3.8) into Eq (3.5), neglecting the nonlinear terms and after parabolizing the equations, we obtain stability equations of three-dimensional, compressible, nonparallel flow along curved, divergent bodies.

As compared to linear stability theory in which the disturbance vector is defined as

$$\boldsymbol{\Psi} = \overline{\boldsymbol{\Psi}}(\zeta)\mathrm{e}^{\mathrm{i}(\alpha\xi + m\eta - \omega t)} \tag{3.10}$$

the amplitude function in parabolic stability theory is a function of both ξ and ζ coordinates due to the growth of the boundary layer, and the wave number α is a function of ξ. On the contrary, in the local primary linear stability theory (Eq (3.10)) the stability of mean flow in a certain position is investigated and the mean flow is regarded to be locally parallel.

The present study is concentrated on the local stability theory. However, we might stress that parabolized stability equations can be derived by generalizing this approach in a straightforward manner. As pointed out in the introduction, results are compared with the experimental data of Stetson et al. (1983) and the numerical parabolic calculation to find the reason for discrepancy between theoretical and experimental results and to find how sensitive are the calculated amplification rates of second mode waves $-\alpha_i$ to physical parameters and the precision of theoretical modeling of the basic flow and stability problem.

In our code it is assumed that the ratio of specific heats is constant

$$\kappa = \frac{c_p}{c_v} = 1.4 \tag{3.11}$$

as well as the Prandtl number. According to Bertolotti (1991), this simplification can have an influence on the amplification rates. The ratio of second

viscosity to the first viscosity is

$$\frac{\lambda_0}{\mu_0} = \frac{2(d-1)}{3} \tag{3.12}$$

where $d = 0.0$ represents the Stokes hypothesis which is valid for monoatomic gases. For polyatomic gases like air $d = 1.2$. In the present investigations we apply the Stokes hypothesis however, in the discussion of obtained results the effect of parametr d on the amplification rate is shown.

The transport coefficients are functions of temperature only (the viscosity μ is assumed to vary according to the Sutherland formula) so their fluctuations can be represented as the first order expansions in temperature

$$\mu = \frac{d\mu_0}{dT}\tau' \qquad \lambda = \frac{d\lambda_0}{dT}\tau' \qquad k = \frac{dk_0}{dT}\tau' \tag{3.13}$$

Mean flow is obtained from boundary layer equations using Mangler's transformation and similarity variables. Finally we obtain the following ordinary differential system of equations

$$\left(\mathbf{A}\frac{d^2}{d\zeta^2} + \mathbf{B}\frac{d}{d\zeta} + \mathbf{C}\right)\boldsymbol{\Psi} = 0 \tag{3.14}$$

where $\mathbf{A}$, $\mathbf{B}$, $\mathbf{C}$ are 5×5 matrices.

We have the following homogeneous boundary conditions at the wall for velocity and temperature amplitude functions

$$\bar{u}(0) = \bar{v}(0) = \bar{w}(0) = \bar{\tau}(0) = 0 \tag{3.15}$$

Disturbances decay exponentially in the region of inviscid flow. To determine the normal mode solution in this region we first transform the system of equations (3.14) into a system of eight first-order differential equations (seeking solutions in outer flow region we assume constant coefficients of Eqs (3.14)) then we solve it using the exponential method. This solution can be written as follows

$$\varphi = \sum_{i=1}^{8} C_i \boldsymbol{q}_i \mathrm{e}^{r_i \zeta} \tag{3.16}$$

where

$$\varphi = \left[\bar{u}, \frac{d\bar{u}}{d\zeta}, \bar{v}, \bar{p}, \bar{\tau}, \frac{d\bar{\tau}}{d\zeta}, \bar{w}, \frac{d\bar{w}}{d\zeta}\right]^{\mathrm{T}}$$

and $\boldsymbol{q}_i$ is a column vector. Eliminating solutions physically impossible (with the real part of r_i greater than zero) and the coefficients C_k, $k = 1, 2, 3, 4$

we obtain four necessary boundary conditions at the far field. The method of introducing outer edge boundary condition into supersonic flow was discussed by Chang (1990). He used linearized Rankin-Hugoniot conditions as the outer boundary conditions in supersonic flow, taking into account the influence of oscillating shock wave on outer boundary conditions. According to Chang, only for problems where the inviscid region between the boundary layer and the shock plays an important role (such as the entropy layer in blunt body flows), it is necessary to replace the free-stream boundary conditions with the adequate shock conditions. Our investigations are carried out for the pointed cone so the influence of oscillating shock wave on boundary edge conditions can be neglected and we can use the results obtained from exponential method as an outer boundary condition.

The linear compressible stability equations are solved using the fourth order accurate two-point scheme which is derived by means of the Euler-Maclaurin formula

$$\varphi^k - \varphi^{k-1} = \frac{h_k}{2}\left(\frac{d\varphi^k}{d\zeta} + \frac{d\varphi^{k-1}}{d\zeta}\right) - \frac{h_k^2}{12}\left(\frac{d^2\varphi^k}{d\zeta^2} - \frac{d^2\varphi^{k-1}}{d\zeta^2}\right) + \mathcal{O}(h_k^5) \qquad (3.17)$$

where $\varphi^k = \varphi(\zeta^k)$.

The final eigenvalue problem is solved using the direct method which is described in detail by Malik et al. (1982).

4. Comparison of experimental and theoretical results

As mentioned before, we based our comparison of theoretical with experimental results on Stetson et al. (1993) stability experiments. The experiments were carried out in a hypersonic wind tunnel operated at a free stream Mach number $\mathrm{Ma}_\infty = 8.0$, stagnation temperature $T_0 = 723\,\mathrm{K}$ and free stream unit Reynolds number $\mathrm{Re}_\infty = 3.28 \cdot 10^6/\mathrm{m}$ under adiabatic condition. Flow around a cone of 7 degrees half angle with the nose radius of $3.81 \cdot 10^{-6}\,\mathrm{m}$ was examined. The radius was so small that the inviscid entropy layer effects were negligible. Under these conditions the Mach number of inviscid flow at the wall is $\mathrm{Ma}_e = 6.8$. Calculations made in the present paper as well as all the quoted results were made for Stetson's wind tunnel parameters.

In Fig.5 the instability characteristics, i.e. spatial amplification rates $-\alpha_i$ of linear stability theory versus dimensionless frequency $(F = \omega/\mathrm{Re})$ obtained numerically by different authors and the experimental measurement of Stetson

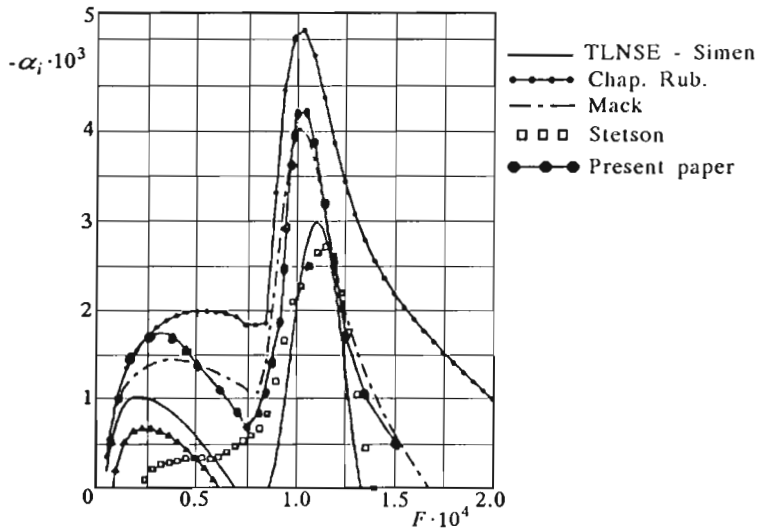

Fig. 5. Instability characteristics obtained numerically by different authors, and the experimental results of Stetson et al. (1983)

et al. (1983) are analyzed. Calculations are obtained for the Reynolds number Re = 1730 ($\mathrm{Re} = \sqrt{U_e \xi / \nu_e}$).

The calculations were made for two-dimensional waves of second modes (which are dominant under the flow conditions assumed) and three-dimensional first mode using spatial theory. From Fig.5 it is seen that discrepancies between the results are big.

The growth rates obtained by Simen and Dallmann (1992) based on the Chapman and Rubesin (1946) similarity solution with the linear viscosity-temperature law ($\mu^* = CT^*$, $C = 0.693873 \cdot 10^{-7}\,\mathrm{kg/(msK)}$) specified strongly overpredict the measured values. The results obtained in the present paper and by Mack (1984) (Mangler flat plate transformation and Sutherland's law) are only in qualitative agreement with Stetson's experimental data. The best agreement is found if the stability calculations are based on the mean flow solutions obtained from the Thin Layer Navier Stokes equations (SLNSE) (cf Simen and Dallmann (1992)). In the TLNSE viscous/inviscid interaction is taken into account. The viscous/inviscid interaction can be expected to be present under the flow conditions assumed, as the shock distance from the wall (in the range where instability waves are amplified) is only about three to seven times longer than the boundary layer edge distance from the wall.

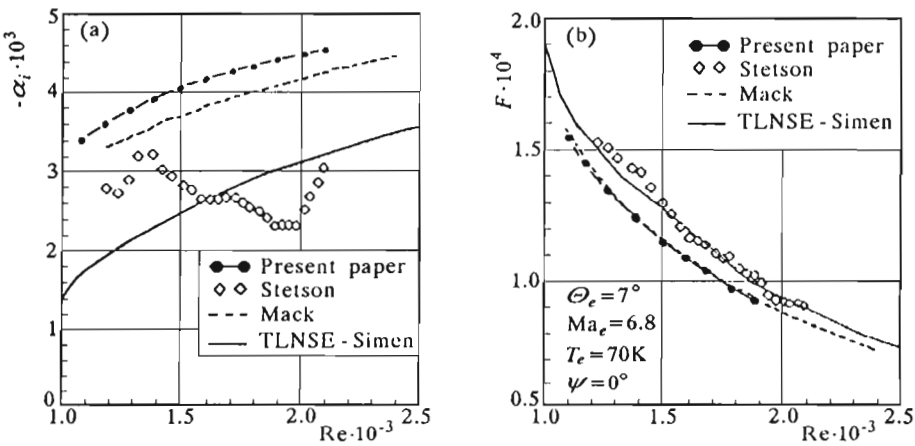

Fig. 6. Amplification rate $-\alpha_i$ (a) and the frequency F (b) of second mode over a vide range of Reynolds numbers. Comparison between theoretical results and experimental data

In Fig.6a the amplification rates $-\alpha_i$ of second mode disturbances over a wide range of Reynolds number obtained in the present paper and by Simen and Dallmann (1992) and Mack (1984) are compared with the experimental data of Stetson. It is seen that amplification rates are uniformly stabilized by the viscous/inviscid interaction taken into account by Simen and Dallmann (1992).

From Fig.5 we see that the range of most unstable frequency in second mode region is relatively well predicted in all theoretical results. In the region of the most unstable frequencies amplification rates obtained for basic state from TLNSE approach almost perfectly match the experimental results. In Fig.6b the frequencies of maximum amplification rate of second mode disturbances versus the Reynolds number are analyzed. The solution based on the TLNSE is again in the best agreement with the experiment.

From Fig.5 and Fig.6 we can draw the conclusion that quantitative discrepancy between experimental and theoretical results in second mode region can be minimalized by a more complete formulation of the equations governing the steady mean flow.

For the first mode (Fig.5) at each frequency the wave angle of most unstable wave must be determined. In the present research these angles have varied from 73 at the lowest frequency to about 35 degrees at the frequency where the second mode waves are dominant. In the first mode region discrepancies between theoretical results and Stetson's measurements are the biggest.

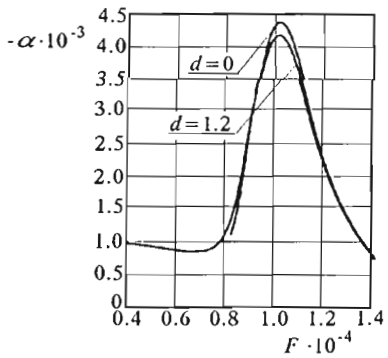

Fig. 7. Instability characteristics obtained for different ratios of second viscosity to first viscosity

In Fig.7 the result obtained in the present contribution for Re=1730 and $Ma_e = 6.8$ and different ratios of second viscosity to first viscosity are analyzed ($d = 0.0$, Stoke's hypothesis valid for monoatomic gases and $d = 1.2$ valid for polyatomic gases). Introducing $d = 1.2$ leads to the 5 percent reduction in maximum amplification rate of second mode.

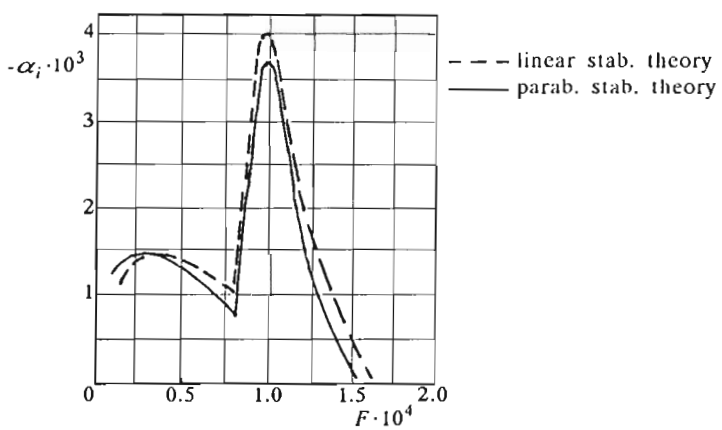

Fig. 8. Amplification rate spectra of maximum amplified first and second mode disturbances obtained by Dallmann (1993) using the linear stability theory and the parabolized theory

In Fig.8 the amplification rate spectra of maximum amplified first and second mode disturbances obtained by Dallman (1993) using the linear stability theory and the parabolized linear stability theory, are compared. We see that the parabolized stability theory gives more stable results.

5. Temperature effect

Stagnation temperature and wall cooling have a strong influence on the growth rates in hypersonic flow. The stabilizing effect of wall cooling on first modes in two and three-dimensional boundary layer were considered by Lekoudis (1979), Balacumar and Reed (1989), Tuliszka-Sznitko (1993). Experimental data which illustrate the influence of cooling on transition onset were collected by Potter and Whitfield (1962), Lysenko and Maslov (1984). In the present investigation we analyze the influence of wall cooling on the second mode instability and the effect of different viscosity-temperature laws on spatial amplification rates.

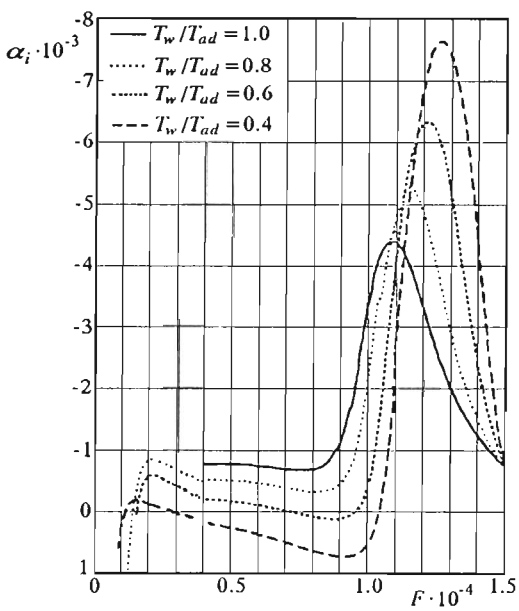

Fig. 9. Amplification rate of second modes in function of frequency for different wall thermal conditions; rotational speed of cone equals zero

Calculations were made for cone of half angle $\Theta = 7$; Reynolds number Re=1730, edge Mach number $\mathrm{Ma}_e = 6.8$ and rotational speeds of the cone around the axis of symmetry $\Omega/U_e = 0.375$ and 0.0. In Fig.9 the amplification rate of second modes in function of frequency is analyzed. Calculations were made for the wall thermal conditions $T_w/T_{ad} = 1.0,\ 0.8,\ 0.6,\ 0.4$ and the rotational speed 0.0 (w and ad denote the wall and adiabatic temperatures, respectively). We see that cooling strongly destabilizes second mode

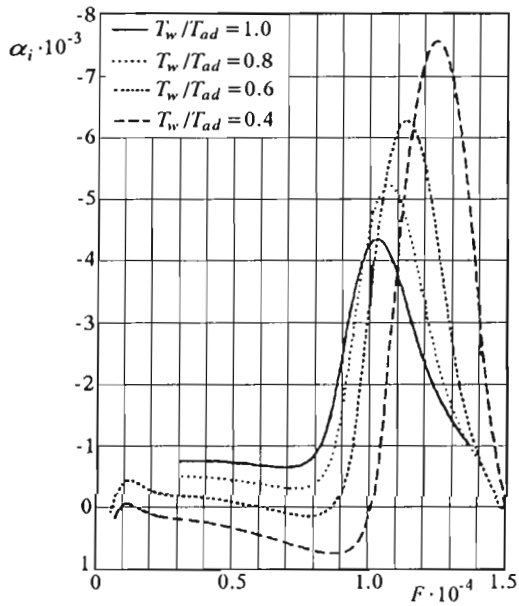

Fig. 10. Amplification rate of second mode in function of frequency, (rotational speed $\Omega/U_e = 0.375$)

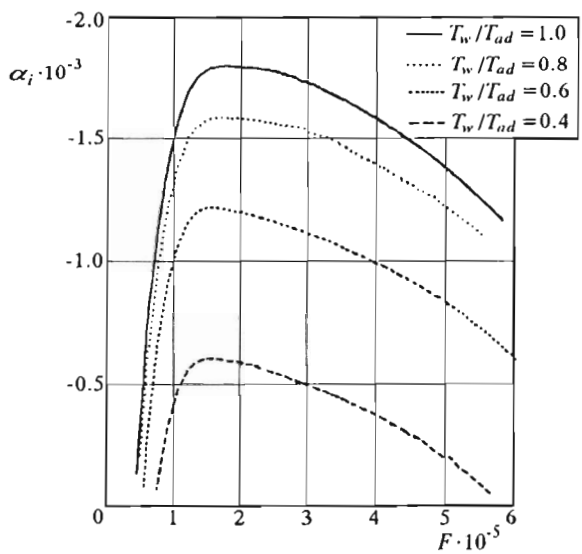

Fig. 11. Amplification rate of first mode in function of frequency for different wall thermal conditions;rotational speed of cone equals zero

disturbances and shifts the most unstable frequency to larger values. Very similar results for second mode disturbances were obtained for the rotational speed $\Omega/U_e = 0.375$ (Fig.10). In Fig.11 the characteristics of first modes for the same case as in Fig.9 are presented. The stabilizing effect of cooling on first modes is seen.

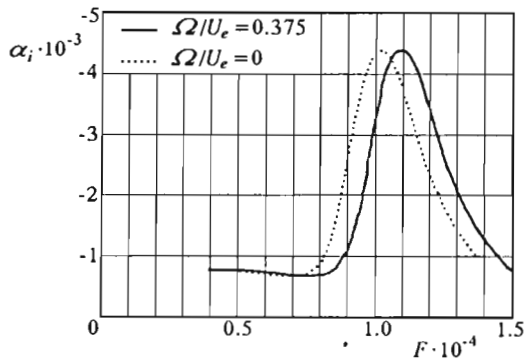

Fig. 12. Instability characteristics of second mode waves obtained for different rotational speed of cone $\Omega/U_e = 0.375$ and 0.0 (adiabatic conditions)

In Fig.12 the comparison of stability characteristics of second modes obtained for rotational speed 0.0 and 0.375 (adiabatic wall) is shown. We see that the influence of crossflow Reynolds number (which is large in the case of $\Omega/U_e = 0.375$) on second mode is insignificant.

The effect of wall thermal conditions on distribution of temperature fluctuations in boundary layer for three-dimensional first mode waves and two-dimensional second mode waves is shown in Fig.13 and Fig.14. The different characters of first and second mode disturbances are clearly seen.

In Fig.15 the influence of viscosity-temperature law on second mode characteristics is shown (line 1 is obtained for the Sutherland formula, line 2 for the linear function $\mu^* = CT^*$, $C = 0.69387 \cdot 10^{-7}$ kg/(msK); asterisk denotes dimensional quantities). More stable results are obtained for the Sutherland law.

6. Conclusions

We have studied the effects of various physical parameters and precision of modeling of mean and perturbated flow on the numerical results (on growth

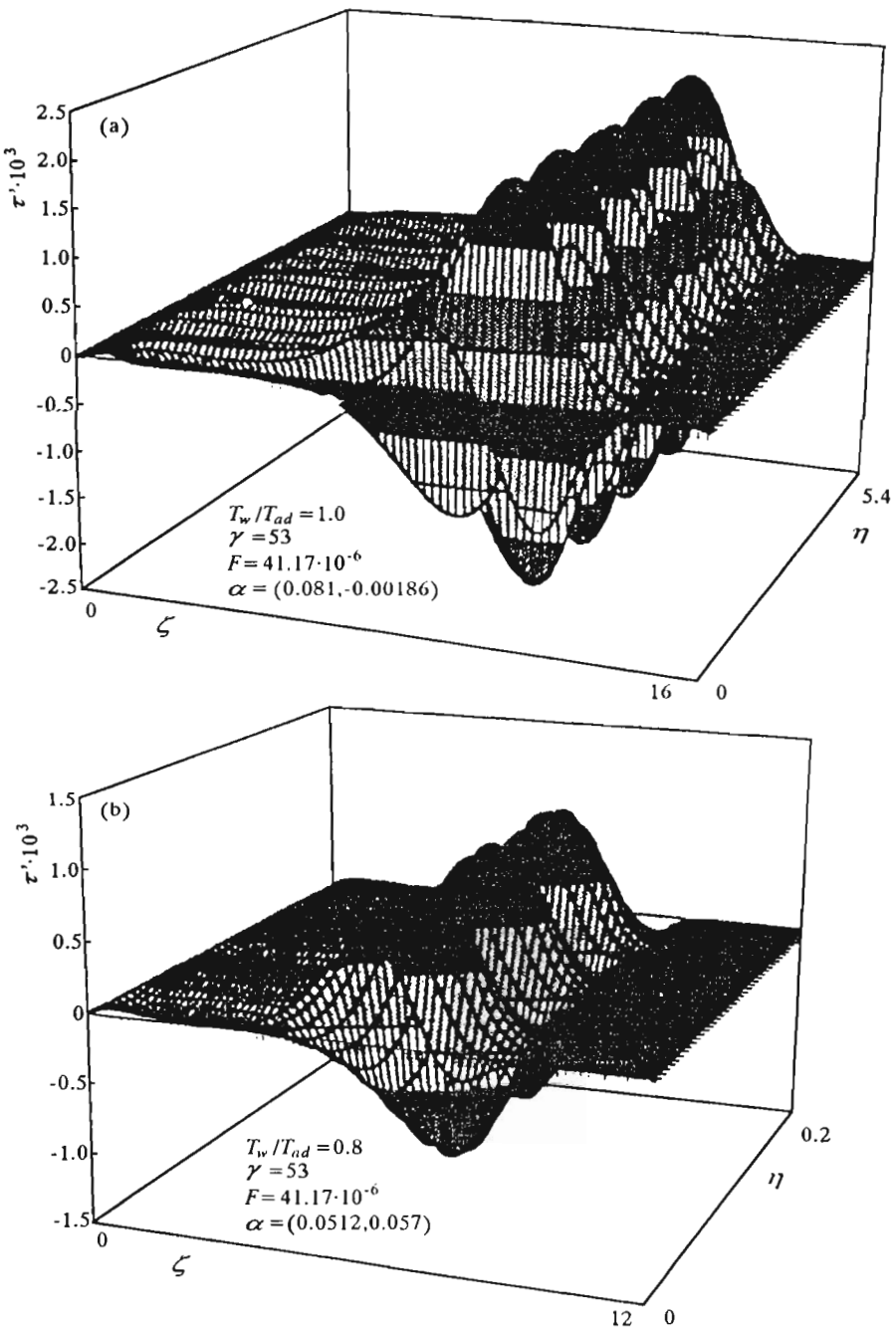

Fig. 13. Temperature fluctuation distribution of first mode for different wall thermal conditions $T_w/T_{ad} = 1.0$ (a), 0.8 (b)

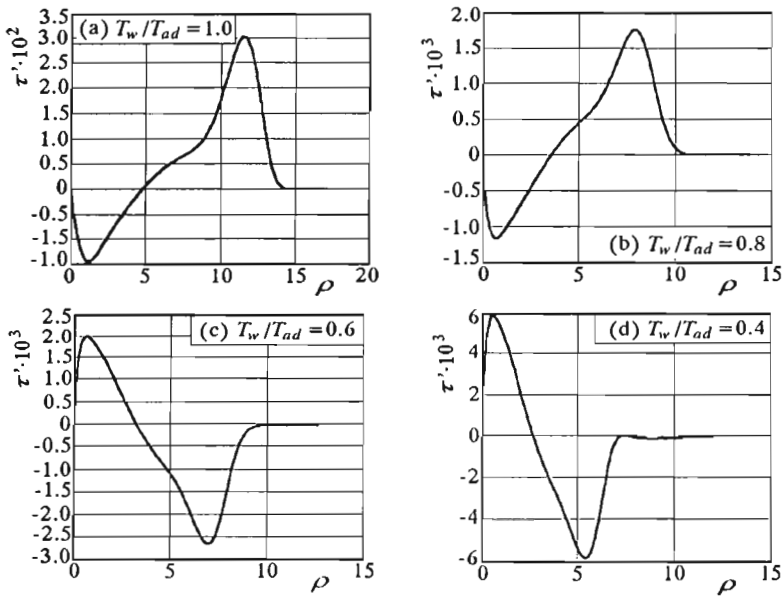

Fig. 14. Temperature fluctuation distribution of second mode for different wall thermal conditions $T_w/T_{ad} = 1.0$ (a), 0.8 (b), 0.6 (c), 0.4 (d)

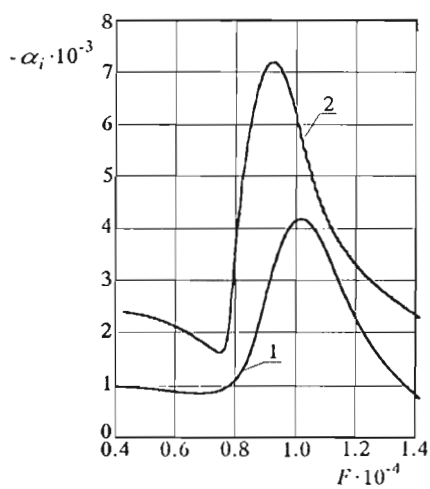

Fig. 15. Influence of viscosity-temperature law on second mode characteristic: 1 – Sutherland formula, 2 – $\mu^* = CT^*$

rate of disturbances) to find the reason of discrepancy between experiment and theory with regard to instabilities in hypersonic flow. From comparison it is seen that markedly better agreement between the linear stability theory and experiment was found when a more complete formulation of steady mean flow equations was taken into account (TLNSE, Simen and Dallmann (1992)). We found that the relation between first and second viscosity had an influence on the instability characteristics. The stabilizing effect of wall cooling on first and destabilizing effect on second mode was shown. It was found that the influence of the viscosity-temperature law on second mode amplification rate is strong.

References

1. BALACUMAR P., REED H., 1989, Stability of Three Dimensional Boundary Layer, *Report of Department of Mechanical and Aerospace Engineering,* ASU, USA
2. BERTOLOTTI F., 1991, Linear and Nonlinear Stability Boundary Layers with Streamwise Varying Properties, Ph. D. Thesis, The Ohio State University, Columbus, USA
3. CHANG C., MALIK M., 1990, Effect of Shock on the Stability of Hypersonic Boundary Layers, *AIAA Paper,* 90-1448
4. CHANG C., MALIK M., 1991, Compressible Stability of Growing Boundary Layers Using Parabolized Stability Equations, *AIAA Paper,* 91-1636
5. CHANG C., MALIK M., 1993, Non-Parallel Stability Compressible Boundary Layer, *AIAA Paper,* 93-2912
6. CHAPMAN D., RUBESIN M., 1949, Temperature and Velocity Profiles in the Compressible Laminar Boundary Layer with Arbitrary Distribution of Surface Temperature, *J. Aero. Sci.,* **16**
7. DALLMANN U., 1993, Local and Nonlocal Instability of Hypersonic Flows, *Space Course TU,* Munchen
8. DEMETRIADES A., 1960, An Experiment on the Stability of Hypersonic Boundary Layers, *J. Fluid Mech.,* **7**
9. DEMETRIADES A., 1977, Laminar Boundary Layer Stability Measurements at Mach 7 Including Wall Temperature Effects, *AFOSR TR-77-1311 Air Force Office of Scientific Research,* Bolling Air Force Base, Washington D.C., USA
10. HERBERT TH., 1991, Boundary Layer Transition Analysis, *AIAA Paper,* 91-0737
11. KENDALL J., 1967, Supersonic Boundary Layer Stability Experiments, *Boundary Layer Transition Steady Grup Meeting,* II, BSD-TR 67-213, USA Air Force

12. KENDALL J., 1975, Wind Tunnel Experiments Relating to Supersonic and Hypersonic Boundary Layer Transition, *AIAA J.*, **13**

13. KOSINOV A., MASLOV D., SHEVELKOV S., 1989, Experimental Study of the Supersonic Boundary Layer Stability on the Cone Cylinder Model, *Laminar Turbulent Transition*, IUTAM-Symp, Toulouse, France

14. KOSINOV A., MASLOV D., SHEVELKOV S., 1990, Experiments on the Stability of Supersonic Laminar Boundary Layers, *J. Fluid Mech.*, **219**

15. LAUFER J., VREBOLOVICH T., 1960, Stability and Transition of a Supersonic Laminar Boundary Layer on an Insulated Flat Plate, *J. Fluid Mech.*, 9

16. LEES L., LIN C., 1946, Investigation of the Stability of the Laminar Boundary Layer in a Compressible Fluid, *NACA Tech. Not.*, 1115

17. LEES L., ROSHODKO E., 1962, Stability of the Compressible Laminar Boundary Layer, *J. Fluid Mech.*, **12**

18. LEKOUDIS S., 1979, The Stability of the Boundary Layer on Swept Wing with Cooling, *AIAA Paper*,79-1495

19. LYSENKO V., MASLOV A., 1984, The Effect of Cooling on Supersonic Boundary Layer Stability, *J. Fluid Mrch.*, **147**

20. MACK L., 1963, The Inviscid Stability of the Compressible Laminar Boundary Layer, *Space Programs Summary*, no. 37-23, Jet Populsion Laboratory, Pasadena, CA

21. MACK L., 1964, The Inviscid Stability of the Compressible Laminar Boundary Layer: Part II, *Space Programs Summary*, no. 37-26, **IV**, Jet Propulsion Laboratory, Pasadena, CA

22. MACK L., 1965, Stability of the Compressible Laminar Boundary Layer according to a Direct Numerical Solution, *AGARDograph*, 97, I

23. MACK L., 1984, Boundary Layer Linear Stability Theory, *AGARDRep.*, 709

24. MACK L., 1987, Stability of Axisymmetric Boundary Layers on Sharp Cones at Hypersonic Mach Numbers, *AIAA Paper*, 87-1413

25. MALIK M., CHANG S., HUSSAINI M., 1982, Accurate Numerical Solution of Compressible Linear Stability Equations, *ZAMP*, **33**

26. POTTER J., WHITFIELD J., 1962, Effect of Slight Nose Bluntness and Roughness on Boundary Layer Transition in Supersonic Flows, *J. Fluid Mech.*, **12**, 4

27. SIMEN M., DALLMANN U., 1992, On the Instability of Hypersonic Flow Past a Pointed Cone – Comparison of Theoretical and Experimental results at Mach 8, *DLR-FB*, 92-2

28. STETSON K., THOMPSON E., DONALDSON J., SILER L., 1983, Laminar Boundary Layer Stability Experiments on a Cone at Mach 8, Part I, *AIAA Paper*, 83-1761

29. TULISZKA-SZNITKO E., 1993, Niestabilność trójwymiarowych warstw przyściennych, *WPP*, **287**

Niestabilność drugich modów

Streszczenie

W pracy analizowany jest metodą symulacji numerycznej rozwój zaburzeń powstających w laminarnej warstwie przyściennej i doprowadzających do przejścia laminarno turbulentnego w przeplywach hipersonicznych. Zaburzenia powstające w hipersonicznych warstwach przyściennych, zwane drugimi modami, są falami dwuwymiarowymi i są silnie destabilizowane przez chlodzenie. Uzyskiwane w wyniku rozwiązania równań niestabilności przeplywu trójwymiarowego i ściśliwego charakterystyki porównane zostały z badaniami eksperymentalnymi Stetsona i rozwiązaniami numerycznymi innych autorów. Badano wplyw różnych parametrów fizycznych oraz modelowania przeplywu podstawowego i zaburzonego na uzyskiwane rezultaty.

Manuscript received June 5, 1995; accepted for print December 15, 1995